

# The Insertion of Heterocumulenes into Zn–H and Zn–OH Bonds of Pyrazolylborate–Zinc Complexes

Michael Rombach,<sup>[a]</sup> Horst Brombacher,<sup>[a]</sup> and Heinrich Vahrenkamp\*<sup>[a]</sup>

*Dedicated to Professor Ernst Anders on the occasion of his 60th birthday*

**Keywords:** Zinc / Pyrazolylborate ligands / Heterocumulenes / Insertion / Hydroxide ligands / Enzyme models

The pyrazolylborate–zinc complexes  $\text{Tp}^{\text{Ph,Me}}\text{Zn-H}$  and  $\text{Tp}^{\text{Ph,Me}}\text{Zn-OH}$  undergo insertion reactions with heterocumulenes.  $\text{CO}_2$ ,  $\text{CS}_2$  and  $\text{RNCS}$  insert into the Zn–H function to yield the corresponding Zn–OCH(O), Zn–SCH(S) and Zn–SCH(NR) complexes. The primary products resulting from the insertion of  $\text{CS}_2$ , COS and  $\text{RNCS}$  into the Zn–OH function undergo rearrangements and subsequent reactions.  $\text{Tp}^{\text{Ph,Me}}\text{Zn-OH}$  and  $\text{CS}_2$  or COS yield  $\text{Tp}^{\text{Ph,Me}}\text{Zn-SH}$  and

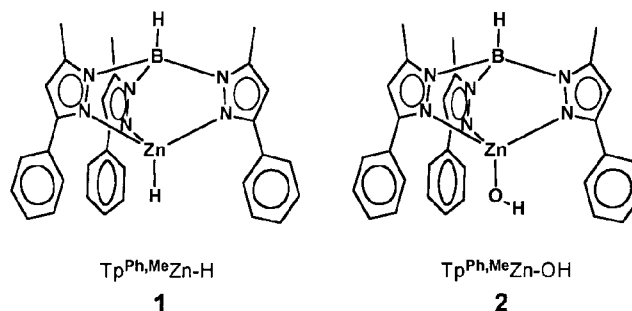
COS or  $\text{CO}_2$ , whereas with  $\text{RNCS}$  the complexes  $\text{Tp}^{\text{Ph,Me}}\text{Zn-SC(O)NHR}$  are formed. In the presence of alcohols these are incorporated in the Zn–OH insertion products:  $\text{CS}_2$ /methanol yields  $\text{Tp}^{\text{Ph,Me}}\text{Zn-SC(S)OMe}$  and  $\text{RNCS}$ /ethanol yields  $\text{Tp}^{\text{Ph,Me}}\text{Zn-SC(NR)OEt}$ . All product types were characterized by X-ray crystallography. The reactions and structures support the four-centre reaction mechanism proposed for hydrolytic zinc enzymes.

## Introduction

Hydrolytic zinc enzymes normally contain a zinc-aqua unit  $\text{L}_n\text{Zn-OH}_2$  in the resting state which becomes active by conversion into the powerful nucleophile  $\text{L}_n\text{Zn-OH}$ .<sup>[1,2]</sup> In one of the simplest zinc-enzyme-catalyzed processes, the hydration of  $\text{CO}_2$  by carbonic anhydrase,<sup>[3]</sup> the primary step consists formally of the insertion of  $\text{CO}_2$  into this Zn–OH function producing an intermediate zinc-bicarbonate complex. Numerous research groups,<sup>[4,5]</sup> including ourselves,<sup>[6–9]</sup> have tried to model the function of carbonic anhydrase using Zn– $\text{OH}_2$  or Zn–OH complexes. Until now, however, zinc-bicarbonate complexes, which seem to be the most labile intermediates, have been elusive. Their existence as intermediates and the mechanistic details of the Zn–OH/ $\text{CO}_2$  reaction have been elucidated in great detail by mechanistic and theoretical investigations.<sup>[3,10]</sup>

Our activities in this field are centred on the easily accessible pyrazolylborate–zinc hydroxide complexes  $\text{Tp}^*\text{Zn-OH}$ , which we have called the Freiburg enzyme model.<sup>[11]</sup> We have described some reactions of these complexes with  $\text{CO}_2$ ,<sup>[6–8]</sup> and related heterocumulenes such as  $\text{CS}_2$  and  $\text{RNCS}$ ,<sup>[7,12]</sup> and we have developed mechanistic proposals for the hydrolytic function of the Zn–OH unit based on preparative and kinetic work<sup>[13]</sup> as well as on theoretical considerations<sup>[12]</sup> and a structure correlation analysis.<sup>[13]</sup>

A characteristic feature of the  $\text{Tp}^*\text{Zn-OH}$ /heterocumulene reactions is that their primary reaction products undergo subsequent reactions, either by proton migration or solvent incorporation.<sup>[6–8,12]</sup> In order to learn more about the possible primary products we therefore looked for a  $\text{Tp}^*\text{Zn}$  complex as a starting material which bears a nucleophilic yet nonprotic ligand X capable of allowing insertion of the heterocumulene into the Zn–X function. We found that Zn–SH or Zn–SR complexes are not suitable for this purpose due to reluctance of the sulfur ligands to undergo Zn–S bond cleavage.<sup>[14,15]</sup> It turned out, however, that the Zn–H function in  $\text{Tp}^*\text{Zn-H}$  complexes has all of the desired characteristics. This paper describes the heterocumulene reactions of  $\text{Tp}^{\text{Ph,Me}}\text{Zn-H}$  (**1**). The related reactions of  $\text{Tp}^{\text{Ph,Me}}\text{Zn-OH}$  (**2**), which have also yielded new insights, are included. The independent chemistry of  $\text{Tp}^{\text{Ph,Me}}\text{Zn-OR}$  complexes which bear the highly nucleophilic and extremely labile alkoxide ligands will be described in a separate paper.<sup>[16]</sup>



<sup>[a]</sup> Institut für Anorganische und Analytische Chemie der Universität Freiburg, Albertstraße 21, 79104 Freiburg, Germany  
 Fax: (internat.) + 49-761/203-6001  
 E-mail: vahrenka@uni-freiburg.de

## Results and Discussion

Reactions of  $\text{Tp}^{\text{Ph,Me}}\text{Zn-H}$ 

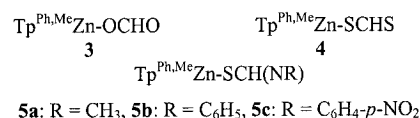
$\text{Tp}^{\text{tBu}}\text{Zn-H}$  was prepared previously by Parkin from  $\text{ZnH}_2$  and the ligand,<sup>[17]</sup> and  $\text{Tp}^{\text{p-Tol,Me}}\text{Zn-H}$  by Kläui from the corresponding fluoride and triethylsilane.<sup>[18]</sup> The reactivity of the former towards protic reagents and alkyl halides had already been studied, as had its reaction with  $\text{CO}_2$  to form  $\text{Tp}^{\text{tBu}}\text{Zn-formate}$ , which was characterized spectroscopically.<sup>[17]</sup>

We chose the Kläui method to prepare **1**. Both the formation of  $\text{Tp}^{\text{Ph,Me}}\text{Zn-F}$  from  $\text{KTp}^{\text{Ph,Me}}$ ,  $\text{Zn}(\text{ClO}_4)_2$  and  $\text{KF}$  and its conversion into **1** with triethylsilane are high yield processes. The hydride complex **1** is remarkably stable. It melts without decomposition above 200 °C, and can be handled for short periods in the open atmosphere. Its  $^1\text{H}$  NMR spectrum in  $\text{CDCl}_3$  shows the hydride resonance at  $\delta = 4.06$ , which is in the range observed for the other two  $\text{Tp}^*\text{Zn-H}$  complexes.

The structure of the hydride complex **1** is displayed in Figure 1. Although an electron density which roughly corresponds to that of a hydrogen atom could be localized at the position given in the figure, it is unrealistic to assign it to the zinc-bound hydride due to the observed distance of 1.9 Å, which is well above the accepted  $\text{Zn-H}$  distance of ca. 1.60 Å.<sup>[19]</sup> Compound **1** shares this feature with  $\text{Tp}^{\text{tBu}}\text{Zn-H}$ ,<sup>[17]</sup> for which the hydride position was also not located but whose  $\text{ZnN}_3\text{H}$  arrangement is practically identical to that in **1**. Thus the main purpose of Figure 1 is to show the encapsulation of the  $\text{Zn-H}$  function by the phenyl groups on the pyrazole rings and to give one representative drawing of the complete pyrazolylborate ligand  $\text{Tp}^{\text{Ph,Me}}$  which is omitted for clarity in all subsequent figures.

$\text{Tp}^{\text{Ph,Me}}\text{Zn-H}$  reacts readily with  $\text{CO}_2$  or  $\text{CS}_2$  in excess at ambient temperature to yield the corresponding formate or dithioformate complexes **3** and **4**. The transfer of the hydridic H atom from zinc to carbon, i.e. the insertion of the heterocumulene into the  $\text{Zn-H}$  function, is obvious

from the NMR spectroscopic data and was confirmed by the structure determinations (see below). Likewise the isothiocyanates  $\text{RNCS}$  ( $\text{R} = \text{methyl, phenyl and } p\text{-nitrophenyl}$ ) are inserted with formation of the corresponding iminothioformates **5a-c**. All three are crystalline solids with high thermal stabilities, whose formate nature is again evident from the formate proton resonances in the  $^1\text{H}$  NMR spectrum.



The structure determinations of **3**, **4** and **5c** revealed the common features and characteristic differences of the species. In all drawings the attachment of the pyrazolylborate ligand to zinc is reduced to the attachment of its nitrogen donors for the purpose of an unobscured view of the heterocumulene-derived ligand. The latter is displayed such that its bond to zinc is vertical and the least-squares plane including its bond to zinc is in the plane of the drawing.

The formate complex **3** (Figure 2) is the first structurally authenticated formate complex in the group of  $\text{TpZn-carboxylate}$  complexes. The attachment of the formate ligand to zinc with a somewhat elongated  $\text{Zn-O1}$  bond and a rather weak, but non-negligible,  $\text{Zn}\cdots\text{O2}$  interaction must be classified as semibidentate. In comparison, the acetate in  $\text{Tp}^{\text{tBu}}\text{Zn-OC(O)Me}$  is clearly monodentate with  $\text{Zn-O1} = 1.86$  Å and  $\text{Zn-O2} = 2.95$  Å.<sup>[17]</sup> The extensive discussion of bidentate bonding of ligands to  $\text{TpZn}$  units<sup>[5,13]</sup> has identified another indicator for the strength of the interaction of the zinc ion with the second donor of the bidentate ligand. This is the position of the pyrazolylborate nitrogen *trans* to this second donor. In the case of **3** this is N2. N2 is not precisely *trans* to O2 ( $\text{N2-Zn-O2} = 169.0^\circ$ ), it is not part of the planar  $\text{ZnOOCH}$  array (displacement 0.20 Å), and its bond to zinc is not longer than the other two  $\text{Zn-N}$  bonds. Thus the formate attachment is actually weakly semibidentate, resembling the nitrate attachment in  $\text{Tp}^{\text{tBu}}\text{Zn-ONO}_2$ .<sup>[20]</sup>

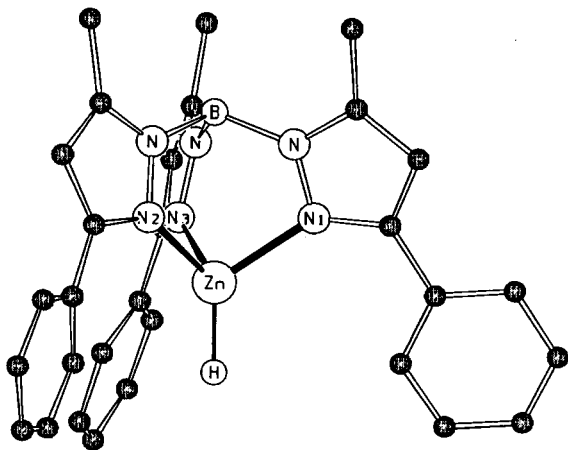


Figure 1. Molecular structure of  $\text{Tp}^{\text{Ph,Me}}\text{Zn-H}$  (**1**); bond lengths:  $\text{Zn-N1}$  2.079(5),  $\text{Zn-N2}$  2.081(4),  $\text{Zn-N3}$  2.054(5) Å

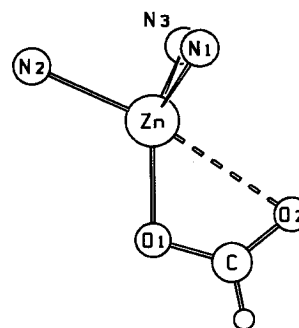


Figure 2. Zinc coordination in  $\text{Tp}^{\text{Ph,Me}}\text{Zn-OCHO}$  (**3**); bond lengths:  $\text{Zn-O1}$  1.918(3),  $\text{Zn}\cdots\text{O2}$  2.642(3),  $\text{Zn-N1}$  2.034(5),  $\text{Zn-N2}$  2.058(4),  $\text{Zn-N3}$  2.068(4),  $\text{O1-C}$  1.277(7),  $\text{O2-C}$  1.208(7) Å; bond angles:  $\text{Zn-O1-C}$  106.6(4),  $\text{O1-C-O2}$  124.2(5)°

The dithioformate complex **4** (Figure 3) is, to the best of our knowledge, the first structurally authenticated classical coordination compound with a dithioformate ligand. In contrast, dithioformate complexes are not uncommon in organometallic chemistry where, as a rule, the dithioformate ligand bridges two metal atoms.<sup>[21]</sup> In **4** the attachment and orientation of the HCS<sub>2</sub> unit is quite similar to that of the HCO<sub>2</sub> unit in **3**. Again, the Zn–S2 interaction is not only obvious from the Zn–S2 distance of 3.02 Å but also from the strict planarity of the Zn–SCHS array and the *trans* arrangement of N3 and S2 with a bond angle of 176.3°. The N3 nitrogen is 0.13 Å above the Zn–SCHS plane, and its Zn–N bond is 0.07 Å longer than the average of the other two Zn–N bonds. The dithioformate ligand itself shows no unusual features, displaying an sp<sup>2</sup> carbon, a short C–S1 single bond and a long C–S2 double bond, in agreement with the semibidentate attachment. Thus the protection in the ligand pocket around zinc allows the labile dithioformate to exist as a stable dithiocarboxylic acid derivative with completely normal bonding parameters.

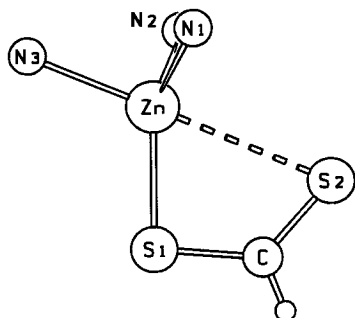


Figure 3. Zinc coordination in  $\text{Tp}^{\text{Ph,Me}}\text{Zn-SCHS}$  (**4**); bond lengths: Zn–S1 2.291(1), Zn···S2 3.019(1), Zn–N1 2.019(2), Zn–N2 2.065(2), Zn–N3 2.111(2), S1–C 1.694(3), S2–C 1.623(3) Å; bond angles: Zn–S1–C 96.64(12), S1–C–S2 126.8(2)°

The iminothioformate ligand in **5c** (Figure 4) shows the closest approximation to a bidentate attachment. The Zn–S bond is longer than that in **4** and the Zn–N7 distance is close to that of a single bond. The array of Zn, S, N1, N7 and C is planar within  $\pm 0.03$  Å, and the N1–Zn–N7 angle is 177.1°. We see no obvious reason why the weakly bound N7 nitrogen in **5c** should be a better donor for zinc than the weakly bound O2 oxygen in **3** or the S2 sulfur in **4**. But while the whole range of attachments between monodentate and symmetrically bidentate is observed for zinc carboxylates<sup>[5,13]</sup> or zinc dithiocarboxylates and related species,<sup>[22,23]</sup> the unsymmetrical four-membered Zn–S–C–N chelate ring as in **5c** seems to be typical for zinc complexes of such ligands, specifically those derived from 2-mercaptopyridine-like heterocycles.<sup>[24–26]</sup> The basic form of the ligand in **5c**, iminothioformic acid HC(SH)(NH), exists only as thioformamide HC(S)NH<sub>2</sub>. Its *N*-substituted derivatives, HC(SH)(NR), represented by the iminothioformate ligand in **5c**, can, however, exist as such under very favourable conditions.<sup>[27]</sup> We are not aware, however, that an anionic ligand of the type HC(S)(NR) has been used in a coordination compound before.

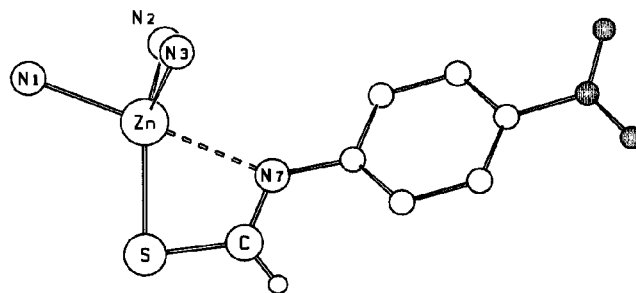


Figure 4. Zinc coordination in  $\text{Tp}^{\text{Ph,Me}}\text{Zn-SCH}(\text{NC}_6\text{H}_4\text{-}p\text{-NO}_2)$  (**5c**); bond lengths: Zn–S 2.341(1), Zn···N7 2.373(3), Zn–N1 2.127(3), Zn–N2 2.048(3), Zn–N3 2.074(3), S–C 1.704(4), N7–C 1.277(5) Å; bond angles: Zn–S–C 83.24(14), Zn–N7–C 91.8(3), S–C–N7 118.7(3)°

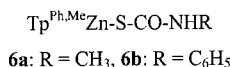
### Reactions of $\text{Tp}^{\text{Ph,Me}}\text{Zn-OH}$

We have previously described reactions of  $\text{Tp}^*\text{Zn-OH}$  complexes with CO<sub>2</sub> in alcohols,<sup>[7,8]</sup> with CS<sub>2</sub> in alcohols<sup>[7]</sup> and in nonprotic solvents,<sup>[12]</sup> and with phenylisothiocyanate.<sup>[7]</sup> We had two reasons to repeat such reactions with  $\text{Tp}^{\text{Ph,Me}}\text{Zn-OH}$  (**2**). Firstly, it was hoped that they would proceed like the reaction of  $\text{Tp}^{\text{Ph,Me}}\text{Zn-H}$  (**1**) without subsequent reactions, thereby giving access to carbonic acid derivatives analogous to the formic acid derivatives **3–5**. Secondly, the favourable crystallization tendency of all  $\text{Tp}^{\text{Ph,Me}}\text{Zn-X}$  complexes should allow for structural comparisons between the formic acid and carbonic acid derived complexes. The first expectation was not fulfilled: all heterocumulene insertions were accompanied by subsequent reactions. The structural comparisons, however, proved to be valuable.

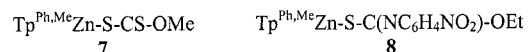
The investigation of the reaction of **2** with CS<sub>2</sub> under nonprotic conditions was initiated by the theoretical prediction that it would lead to  $\text{Tp}^{\text{Ph,Me}}\text{Zn-SH}$  and COS.<sup>[12]</sup> To our surprise this was actually the case and has resulted in a fruitful collaboration with the theoretical group of Anders.<sup>[12]</sup> In water-free dichloromethane, **2** and a stoichiometric amount of CS<sub>2</sub> were converted quantitatively to  $\text{Tp}^{\text{Ph,Me}}\text{Zn-SH}$ <sup>[14]</sup> and COS within 12 hours at room temperature. The COS resulting from this reaction in toluene was identified by mass spectrometry. Thereby it was found that under these conditions it was contaminated with CO<sub>2</sub>, leading to the assumption that COS itself undergoes the same reaction. This was verified subsequently by the isolation of  $\text{Tp}^{\text{Ph,Me}}\text{Zn-SH}$ , again in a high yield, from the reaction of **2** with COS. The theoretical analysis of these interconversions,<sup>[12]</sup> whose insertion mechanism and proton migrations are of relevance for the functionality of the zinc enzyme carbonic anhydrase, will be published separately.<sup>[28]</sup> In the context of the present work these findings confirm the observation that insertions into the Zn–OH function of  $\text{Tp}^*\text{Zn-OH}$  complexes will be accompanied by molecular rearrangements.

The simplest of these rearrangements, an OH/NH tautomerization, was now observed when reacting **2** with isothiocyanates in water-free dichloromethane. Methyl and

phenyl isothiocyanate yielded the thiocarbamate complexes **6a** and **6b**, respectively. Insertion alone would result in the iminothiocarbonate complexes  $\text{Tp}^{\text{Ph,Me}}\text{Zn}-\text{SC}(\text{NR})\text{OH}$ . The migration of the OH proton to the more basic nitrogen should be a facile process.



Esterification rather than proton migration was the subsequent reaction when performing such insertions in the presence of alcohols. As observed before for a related system,<sup>[7]</sup> CS<sub>2</sub> was inserted in the presence of one equivalent of methanol to yield the xanthogenate complex **7**. The insertion of *p*-nitrophenyl isothiocyanate in ethanol-stabilized chloroform produced the iminothiocarbonate complex **8**. Both results can be interpreted as an esterification of the primary insertion products  $\text{Tp}^{\text{Ph,Me}}\text{Zn}-\text{S}-\text{CS}-\text{OH}$  and  $\text{Tp}^{\text{Ph,Me}}\text{Zn}-\text{S}-\text{C}(\text{NR})-\text{OH}$ . However, initial replacement of OH by OR to form  $\text{Tp}^{\text{Ph,Me}}\text{Zn}-\text{OR}$  as the species which is then subjected to insertion, cannot be ruled out with complete certainty. Although the alkoxides  $\text{Tp}^*\text{Zn}-\text{OR}$  exist only in extremely low concentrations as equilibrium species of  $\text{Tp}^*\text{Zn}-\text{OH}$  in alcohol solvents,<sup>[29]</sup> they might be the precursors of the product complexes **7** and **8**.



The molecular structure of the thiocarbamate complex **6a** (Figure 5) corresponds to that of the related thiocarboxylate complexes  $\text{Tp}^*\text{Zn}-\text{S}-\text{CO}-\text{R}$ ,<sup>[30]</sup> and the ligand attachment, orientation and bond lengths are quite similar to the only other structurally characterized zinc complex of this type, a bis(thiocarbamate)-bis(amine) zinc complex.<sup>[31]</sup> The long C...O distance indicates a very weak C...O interaction, as does the uniformity of the Zn–N distances. The fact that the carbamate oxygen rather than the carbamate nitrogen is in the vicinity of the zinc ion points to steric rather than electronic reasons for the arrangement of the thiocarbamate ligand. The Zn–S–C–O array is only roughly planar ( $\pm 0.08$  Å) and N2 is displaced 0.4 Å from this plane. The bond lengths and angles within the thiocar-

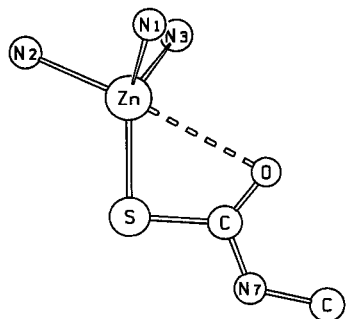


Figure 5. Zinc coordination in  $\text{Tp}^{\text{Ph,Me}}\text{Zn}-\text{S}-\text{CO}-\text{NHMe}$  (**6a**); bond lengths: Zn–S 2.244(1), Zn...O 2.869(4), Zn–N1 2.085(3), Zn–N2 2.091(3), Zn–N3 2.044(3), S–C 1.734(5), C–O 1.223(5), C–N7 1.348(6) Å; bond angles: Zn–S–C 94.15(17), S–C–O 124.1(4)°

bamate ligand are normal, therefore the attachment of the thiocarbamate ligand to zinc causes no unusual bonding features for the metal ion or for the ligand.

The structure of the xanthogenate complex **7** (Figure 6) complements that of  $\text{Tp}^{\text{Cum,Me}}\text{Zn}-\text{S}-\text{CS}-\text{OEt}$ .<sup>[7]</sup> Unlike in **6a** the sterically more demanding OR unit of the xanthogenate ligand is oriented towards zinc rather than the second sulfur atom. This points to a Zn...O interaction, as does the Zn...O distance which corresponds to that in the formate complex **3**. Likewise, the strict planarity of all five atoms of the Zn–S–CS–O unit and the displacement of N1 by 0.25 Å from this plane correspond to the situation in **3**, grouping the xanthogenate ligand in the weakly semibidentate class. The bonding details of the MeOCS<sub>2</sub> ligand

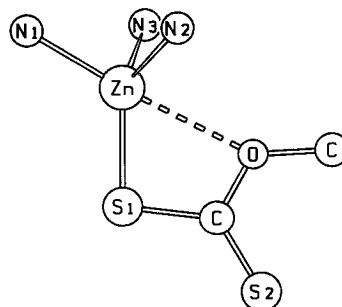


Figure 6. Zinc coordination in  $\text{Tp}^{\text{Ph,Me}}\text{Zn}-\text{S}-\text{CS}-\text{OMe}$  (**7**); bond lengths: Zn–S1 2.244(3), Zn...O 2.685(3), Zn–N1 2.051(7), Zn–N2 2.036(8), Zn–N3 2.031(7), S1–C 1.72(1), C–S2 1.62(1), C–O 1.37(1) Å; bond angles: Zn–S1–C 97.5(4), S1–C–O 111.2(7)°

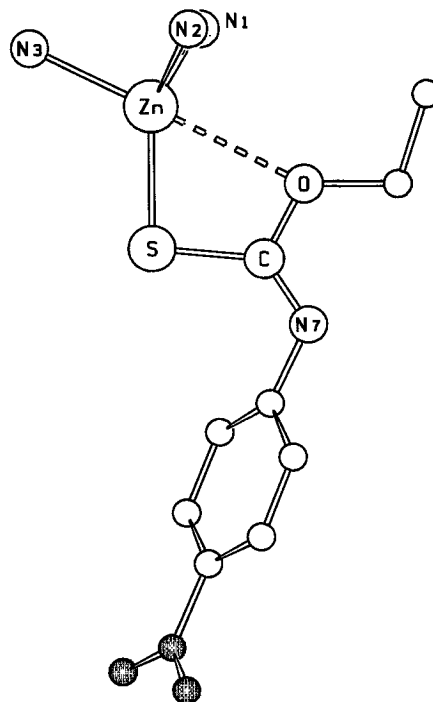


Figure 7. Zinc coordination in  $\text{Tp}^{\text{Ph,Me}}\text{Zn}-\text{S}-\text{C}(\text{NR})-\text{OEt}$  (**8**); bond lengths: Zn–S 2.254(2), Zn...O 2.680(5), Zn–N1 2.038(7), Zn–N2 2.034(6), Zn–N3 2.087(7), S–C 1.75(1), C–N7 1.27(1), C–O 1.35(1) Å; bond angles: Zn–S–C 95.8(3), S–C–O 112.1(6)°

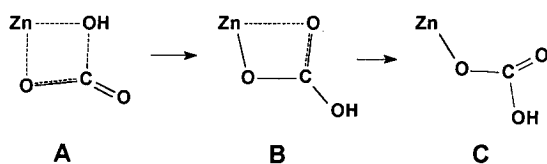
in **7** are in full agreement with those of the EtOCS<sub>2</sub> ligand, as discussed in comparison with reference compounds for Tp<sup>Cum,Me</sup>Zn–S–CS–OEt.<sup>[7]</sup>

The iminothiocarbonate ligand in **8** (Figure 7) seems to represent a type of ligand that has been unknown in coordination chemistry so far. Its attachment to zinc is quite similar to that of the xanthogenate ligand in **7**, however. This extends to the molecular details of the ligand as well as to its zinc–ligand interactions. Although the Zn···O contact shows the same interatomic distance as that in **7**, it seems to be somewhat stronger, as evidenced by the extension of the Zn–N3 bond *trans* to the Zn···O interaction, the O–Zn–N3 angle of 178.3° and the position of N3 in the plane defined by the Zn–S–C–O unit. It is noteworthy to compare the orientations of the *p*-nitrophenyl groups in **5c** (Figure 4) and **8**, which again point to the fact that electronic rather than steric influences determine the preferred donor for the weak interaction with the zinc ion.

### Mechanistic Implications

The theoretical and mechanistic analysis of the key reaction of hydrolytic zinc enzymes – the nucleophilic attack of the Zn–OH function at the electrophilic centre of the substrate, specifically CO<sub>2</sub> – has led to the proposal that a four-centre mechanism prevails.<sup>[3,11,12]</sup> In this process, as displayed below for the hydration of CO<sub>2</sub>, the zinc-bound OH is a leaving group, and the transformation of CO<sub>2</sub> to bicarbonate proceeds via the bidentate to the monodentate attachment of the latter.

The insertions of the heterocumulenes described here result in bonding situations which model transient bonding situations along the reaction coordinate of the enzymatic process. Three stages can be identified: Situation **A** is represented by the structures of **7** and **8** which contain the weakly bound oxygen donor as an alkoxide function which models the OH function of the enzyme. The substrate (CO<sub>2</sub> being modelled by CS<sub>2</sub> or RNCS) is attached in a four-centre fashion, and the Zn–OR bond is noticeably weakened. Situation **B** results from **A** either by proton transfer (Lipscomb mechanism<sup>[3]</sup>) or by internal rotation (Lindskog mechanism<sup>[3]</sup>). It is best represented by the structure of **5c** with a rather strong Zn–N interaction. The transition from situation **B** to **C** with a progressive weakening of the Zn···O interaction is represented by the structures of **3**, **6a** and **4**, in that order. While the formate ligand in **3** is an example of semibidentate coordination, the thiocarbamate ligand in **6a** is close to being monodentate. The six structures described here do not represent situation **C** (strictly monodentate). The latter is, however, approximated in our complexes Tp<sup>Ph,Me</sup>Zn–SC(O)CH<sub>3</sub><sup>[30]</sup> and Tp<sup>tBu,Me</sup>Zn–OC(O)OCH<sub>3</sub>.<sup>[6]</sup>



We have discussed in detail the changes in the coordination sphere of zinc upon the transition from **A** to **B**, as modelled by Tp<sup>\*</sup>Zn(X)(Y) complexes.<sup>[11]</sup> The six structures in this paper provide further examples for this discussion which describes the path from the substrate attachment to the OH elimination as a transition along the Berry coordinate of the Berry pseudorotation of AB<sub>5</sub> molecules. They represent various stages of the interconversion between square-pyramidal and trigonal-bipyramidal coordination of zinc, as can be seen from their trans N–Zn–X angles (see Figure 2–7) ranging from 169–178°. Likewise their “percentage of trigonal-bipyramidal” values, as calculated by the dihedral angle method<sup>[13]</sup> range from 62% (**6a**) to 72% (**4**). A detailed discussion of these features, however, is not appropriate, as the distortions in the coordination sphere of zinc are spread over a range which is too narrow.

In summary, the chemical interconversions described in this paper have shown that the strong Zn–X nucleophiles Zn–H and Zn–OH can attack and incorporate all classical heterocumulenes and thereby model the biological Zn–OH/CO<sub>2</sub> chemistry. The structures of the resulting complexes have provided valuable insights into the molecular transformations occurring during the hydration of CO<sub>2</sub> as catalyzed by the zinc enzyme carbonic anhydrase.

### Experimental Section

**General:** For general working and measuring procedures, see ref.<sup>[32]</sup> All reactions were performed in air- and water-free solvents under an inert atmosphere. Tp<sup>Ph,Me</sup>Zn–OH<sup>[33]</sup> and COS<sup>[34]</sup> were prepared by the published procedures.

**Tp<sup>Ph,Me</sup>Zn–F:** A solution of Zn(ClO<sub>4</sub>)<sub>2</sub>·6H<sub>2</sub>O (1.43 g, 3.83 mmol) in 20 mL of methanol was added with stirring to a solution of KTp<sup>Ph,Me</sup><sup>[33]</sup> (2.00 g, 3.83 mmol) in 100 mL of dichloromethane. A colourless precipitate was formed. After 2 h of stirring a solution of KF (222 mg, 3.83 mmol) in 10 mL of methanol was added. After stirring for 20 h and filtration the solution was reduced to 50 mL in vacuo and kept at –20 °C. Tp<sup>Ph,Me</sup>Zn–F (1.83 g, 84%) precipitated as colourless crystals, m.p. 244 °C. C<sub>30</sub>H<sub>28</sub>BFN<sub>6</sub>Zn (567.8): calcd: C 63.46, H 4.97, N 14.80, Zn 11.50; found C 62.44, H 4.92, N 14.51, Zn 11.69. <sup>1</sup>H NMR (CDCl<sub>3</sub>): δ = 2.53 [s, 9 H, Me(pz)], 6.22 [s, 3 H, H(pz)], 7.33–7.49 (m, 9 H, Ph), 7.91 (d, *J* = 7.4 Hz, 6 H, Ph). <sup>19</sup>F NMR (CDCl<sub>3</sub>): δ = 219.6.

**1:** A solution of Tp<sup>Ph,Me</sup>Zn–F (1.50 g, 2.64 mmol) and Et<sub>3</sub>SiH (4.2 mL, 3.07 g, 26.0 mmol) in 25 mL of toluene was heated to reflux for 2 days. Upon cooling to room temp. the product was precipitated. All volatiles were removed in vacuo, and the residue was recrystallized from hot toluene, yielding 1.31 g (90%) of **1** as colourless crystals, m.p. 239 °C. C<sub>30</sub>H<sub>29</sub>BN<sub>6</sub>Zn (549.8): calcd: C 65.54, H 5.38, N 15.29, Zn 11.89; found C 64.72, H 5.37, N 14.75, Zn 11.79. <sup>1</sup>H NMR (CDCl<sub>3</sub>): δ = 2.47 [s, 9 H, Me(pz)], 4.06 (s, 1 H, ZnH), 6.17 [s, 3 H, H(pz)], 7.19–7.36 (m, 9 H, Ph), 7.72 (d, *J* = 8.0 Hz, 6 H, Ph).

**3:** CO<sub>2</sub> gas, which was dried by passing through a suspension of P<sub>2</sub>O<sub>5</sub> in toluene, was bubbled through a solution of **1** (200 mg, 0.36 mmol) in 30 mL of toluene for 1 h. Evaporation to dryness and recrystallization from hot acetonitrile yielded 164 mg (76%) of **3** as colourless crystals, m.p. 252 °C. C<sub>31</sub>H<sub>29</sub>BN<sub>6</sub>O<sub>2</sub>Zn (593.8):

calcd: C 62.70, H 4.92, N 14.15; found C 62.44, H 4.92, Zn 14.18.  $^1\text{H}$  NMR ( $\text{CDCl}_3$ ):  $\delta$  = 2.53 [s, 9 H, Me(pz)], 6.21 [s, 3 H, H(pz)], 7.34 (m, 9 H, Ph), 7.58 (m, 7 H, Ph and  $\text{HCO}_2$ ).

**4:** A solution of **1** (100 mg, 0.18 mmol) and  $\text{CS}_2$  (138 mg, 1.82 mmol) in 15 mL of toluene was stirred at 40 °C for 16 h. Evaporation to dryness and recrystallization from hot acetonitrile yielded 97 mg (85%) of **4** as pale yellow crystals, m.p. 204 °C.  $\text{C}_{31}\text{H}_{29}\text{BN}_6\text{S}_2\text{Zn}$  (625.9): calcd: C 59.48, H 4.67, N 13.43, S 10.25; found C 59.67, H 4.71, N 13.70, S 9.98.  $^1\text{H}$  NMR ( $\text{CDCl}_3$ ):  $\delta$  = 2.56 [s, 9 H, Me(pz)], 6.17 [s, 3 H, H(pz)], 7.32 (m, 9 H, Ph), 7.53 (m, 6 H, Ph), 10.24 (s, 1 H,  $\text{HCS}_2$ ).

**5a:** Like **4**, from **1** (200 mg, 0.36 mmol) and  $\text{CH}_3\text{NCS}$  (27 mg, 0.36 mmol). Yield 118 mg (52%) of **5a** as colourless crystals, m.p. 214 °C.  $\text{C}_{32}\text{H}_{32}\text{BN}_7\text{SZn}$  (622.9): calcd: C 61.70, H 5.18, N 15.74, S 5.15; found C 62.10, H 5.26, N 16.09, S 4.76.  $^1\text{H}$  NMR ( $\text{CDCl}_3$ ):  $\delta$  = 1.60 (s, 3 H, NMe), 2.55 [s, 9 H, Me(pz)], 6.17 [s, 3 H, H(pz)], 7.30 (m, 9 H, Ph), 7.63 (m, 7 H, Ph and HC).

**5b:** A solution of **1** (200 mg, 0.36 mmol) and  $\text{C}_6\text{H}_5\text{NCS}$  (49 mg, 0.36 mmol) in 30 mL of toluene was heated to reflux for 15 h. Evaporation to dryness and recrystallization from hot acetonitrile yielded 164 mg (66%) of **5b** as colourless crystals, m.p. 181 °C.  $\text{C}_{37}\text{H}_{34}\text{BN}_7\text{SZn}$  (685.0): calcd: C 64.88, H 5.00, N 14.31, S 4.68; found C 64.34, H 4.99, N 14.23, S 4.33.  $^1\text{H}$  NMR ( $\text{CDCl}_3$ ):  $\delta$  = 2.56 [s, 9 H, Me(pz)], 5.59 (m, 3 H, Ph-NCS), 6.14 [s, 3 H, H(pz)], 6.72 (m, 2 H, Ph-NCS), 7.24 (m, 9 H, Ph), 7.54 (m, 6 H, Ph), 7.72 (s, 1 H, HC).

**5c:** A solution of **1** (200 mg, 0.36 mmol) and  $p\text{-NO}_2\text{-C}_6\text{H}_4\text{NCS}$  (66 mg, 0.36 mmol) in 30 mL of acetonitrile was stirred for 15 h. Evaporation to 15 mL in vacuo and cooling to –20 °C resulted in the crystallization of 173 mg (65%) of yellow **5c**, m.p. 239 °C.  $\text{C}_{37}\text{H}_{33}\text{BN}_8\text{O}_2\text{SZn}$  (730.0): calcd: C 60.88, H 4.56, N 15.35, S 4.39;

found C 60.92, H 4.59, N 15.57, S 4.21.  $^1\text{H}$  NMR ( $\text{CDCl}_3$ ): 2.57 [s, 9 H, Me(pz)], 5.64 (d,  $J$  = 8.2 Hz, 2 H,  $\text{C}_6\text{H}_4$ ), 6.15 [s, 3 H, H(pz)], 7.24 (m, 9 H, Ph), 7.50 (m, 6 H, Ph), 7.64 (d,  $J$  = 8.2 Hz, 2 H,  $\text{C}_6\text{H}_4$ ), 7.81 (s, 1 H, HC).

**Reaction of 2 with  $\text{CS}_2$ :** A mixture of **2** (25.0 mg, 44  $\mu\text{mol}$ ) and  $\text{CS}_2$  (336 mg, 4.42 mmol) in 5 mL of toluene under an atmosphere of argon in a sealed 10 mL flask was stirred for 40 h. GC-MS analysis of samples taken from the gas phase with a syringe showed them to contain  $\text{CO}_2$  and COS in about a 1:2 ratio.

**$\text{Tp}^{\text{Ph,Me}}\text{Zn-SH}$  from **2** and  $\text{CS}_2$ :** A solution of **2** (250 mg, 0.44 mmol) and  $\text{CS}_2$  (37.0 mg, 0.49 mmol) in 20 mL of dichloromethane was stirred for 16 h. Evaporation to dryness and recrystallization from acetonitrile yielded 157 mg (61%) of  $\text{Tp}^{\text{Ph,Me}}\text{Zn-SH}$ .<sup>[14]</sup>

**$\text{Tp}^{\text{Ph,Me}}\text{Zn-SH}$  from **2** and COS:** COS gas was passed for 15 min through a solution of **2** (250 mg, 0.44 mmol) in 20 mL of dichloromethane/toluene (4:1). After stirring for 15 h, evaporation to dryness and recrystallization from acetonitrile yielded 183 mg (71%) of  $\text{Tp}^{\text{Ph,Me}}\text{Zn-SH}$ .<sup>[14]</sup>

**6a:** A solution of **2** (250 mg, 0.44 mmol) and  $\text{CH}_3\text{NCS}$  (32.3 mg, 0.44 mmol) in 20 mL of dichloromethane was heated to reflux for 40 h. Evaporation to dryness and recrystallization from benzene yielded 266 mg (84%) of **6a** as colourless crystals, m.p. 184 °C.  $\text{C}_{32}\text{H}_{32}\text{BN}_7\text{OSZn}\cdot\text{C}_6\text{H}_6$  (638.9 + 78.1): calcd: C 63.65, H 5.34, N 13.67, S 4.47; found C 63.43, H 5.33, N 13.77, S 4.62.  $^1\text{H}$  NMR ( $\text{CDCl}_3$ ):  $\delta$  = 1.91 (s, 3 H,  $\text{NCH}_3$ ), 2.52 [s, 9 H, Me(pz)], 4.90 (s, 1 H, NH), 6.13 [s, 3 H, H(pz)], 7.30 (m, 15 H, Ph +  $\text{C}_6\text{H}_6$ ), 7.67 (m, 6 H, Ph).

**6b:** Like **6a** from **2** (250 mg, 0.44 mmol) and  $\text{C}_6\text{H}_5\text{NCS}$  (59.7 mg, 0.44 mmol). Yield 290 mg (77%) of **6b** as colourless crystals, m.p.

Table 1. Crystallographic data

	<b>1</b>	<b>3</b>	<b>4</b>	<b>5c</b>	<b>6a</b>	<b>7</b>	<b>8</b>
Molecular mass	$\text{C}_{30}\text{H}_{29}\text{-BN}_6\text{Zn}$	$\text{C}_{31}\text{H}_{29}\text{-BN}_6\text{O}_2\text{Zn}$	$\text{C}_{31}\text{H}_{29}\text{-BN}_6\text{S}_2\text{Zn}$	$\text{C}_{37}\text{H}_{33}\text{-BN}_8\text{O}_2\text{SZn}$	$\text{C}_{32}\text{H}_{32}\text{-BN}_7\text{OSZn}\cdot\text{C}_6\text{H}_6$	$\text{C}_{32}\text{H}_{31}\text{-BN}_6\text{OS}_2\text{Zn}$	$\text{C}_{39}\text{H}_{37}\text{-BN}_8\text{O}_3\text{SZn}\cdot\text{CH}_2\text{Cl}_2$
Crystal size [mm]	549.8	593.8	625.9	730.0	717.0	656.0	858.9
Space group	$P\bar{1}$	$P\bar{1}$	$P2_1/n$	$P\bar{1}$	$P-1$	$P2_1/c$	$P2_1/c$
$Z$	2	2	4	2	2	4	4
$a$ [Å]	11.685(2)	11.840(6)	10.016(1)	9.540(2)	11.551(2)	12.575(1)	12.076(3)
$b$ [Å]	12.194(2)	12.108(6)	15.644(2)	13.367(3)	12.234(2)	23.533(2)	23.142(6)
$c$ [Å]	15.451(2)	12.448(5)	18.912(2)	14.981(4)	15.261(2)	11.416(1)	14.448(4)
$\alpha$ [°]	83.83(3)	115.772(9)	90	67.735(4)	69.137(3)	90	90
$\beta$ [°]	84.99(3)	108.802(9)	95.781(2)	77.237(5)	84.569(3)	111.952(2)	92.611(6)
$\gamma$ [°]	64.99(3)	98.909(7)	90	87.478(5)	63.035(3)	90	90
$V$ [Å <sup>3</sup> ]	1981.4(7)	1427.3(11)	2948.4(5)	1722.6(7)	1790.4(5)	3133.4(6)	4034(2)
$d(\text{calcd.})$ [g·cm <sup>-3</sup> ]	0.95	1.38	1.41	1.41	1.33	1.39	1.41
$\mu(\text{Mo-K}\alpha)$ [mm <sup>-1</sup> ]	0.64	0.90	1.01	0.82	0.79	0.95	0.84
$hkl$ range	$h$ : –13 to 14 $k$ : 0 to 15 $l$ : 0 to 15	$h$ : –15 to 15 $k$ : –15 to 4 $l$ : –13 to 13	$h$ : –13 to 13 $k$ : –20 to 20 $l$ : –24 to 17	$h$ : –12 to 12 $k$ : –17 to 17 $l$ : –19 to 19	$h$ : –15 to 15 $k$ : –16 to 15 $l$ : –20 to 20	$h$ : –16 to 16 $k$ : –30 to 31 $l$ : –14 to 15	$h$ : –16 to 15 $k$ : –30 to 30 $l$ : –19 to 19
Measured reflections	8119	4289	18352	15817	16506	28597	36370
Independent reflections	7737	4279	7019	7891	8447	7647	9789
Observed refl. [ $I > 2\sigma(I)$ ]	4548	3070	3890	3649	3911	2066	2595
Parameters	469	370	370	451	442	389	505
Refined reflections	7737	4279	7019	7891	8447	7647	9789
$R_1(\text{obs.refl.})$	0.075	0.074	0.041	0.056	0.054	0.086	0.089
$wR_2(\text{all refl.})$	0.228	0.196	0.096	0.146	0.154	0.342	0.288
Residual electron density [e/Å <sup>3</sup> ]	+1.0/–0.6	+1.5/–1.5	+0.4/–0.4	+0.7/–0.6	+0.5/–0.6	+0.7/–0.7	+0.7/–1.1

188 °C.  $C_{37}H_{34}BN_7OSZn \cdot 2C_6H_6$  (701.0 + 156.2): calcd: C 68.66, H 5.41, N 11.44, S 3.74; found C 68.60, H 5.53, N 11.15, S 3.93.  $^1H$  NMR ( $CDCl_3$ ):  $\delta$  = 2.53 [s, 9 H, Me(pz)], 6.17 [s, 3 H, H(pz)], 6.66 (d,  $J$  = 8.1 Hz, 2 H, NPh), 6.86 (m, 1 H, NPh), 7.04 (m, 2 H, NPh), 7.22 (m, 9 H, Ph), 7.35 (s, 12 H,  $C_6H_6$ ), 7.61 (m, 6 H, Ph).

**7:** A solution of **2** (250 mg, 0.44 mmol),  $CS_2$  (37.0 mg, 0.49 mmol) and  $CH_3OH$  (15.6 mg, 0.49 mmol) in 20 mL of dichloromethane was stirred for 16 h. Evaporation to dryness and recrystallization from acetonitrile yielded 228 mg (79%) of **7** as colourless crystals, m.p. 222 °C.  $C_{32}H_{31}BN_6OS_2Zn$  (656.0): calcd: C 58.59, H 4.76, N 12.81, S 9.78; found C 58.67, H 4.84, N 12.81, S 9.98.  $^1H$  NMR ( $CDCl_3$ ):  $\delta$  = 2.55 [s, 9 H, Me(pz)], 2.64 (s, 3 H, OMe), 6.16 [s, 3 H, H(pz)], 7.31 (m, 9 H, Ph), 7.53 (m, 6 H, Ph).

**8:** A solution of **2** (250 mg, 0.44 mmol) and  $p\text{-NO}_2\text{-C}_6\text{H}_4\text{NCS}$  (79.6 mg, 0.44 mmol) in 40 mL of chloroform containing ca. 1% of ethanol as a stabilizer was heated to reflux for 40 h. All volatiles were removed in vacuo, and the residue was dissolved in 10 mL of  $n$ -heptane/dichloromethane (4:1). Slow evaporation of the dichloromethane resulted in the precipitation of 145 mg (42%) of **8** as yellow crystals which lost the solvent of crystallization upon drying in vacuo, m.p. 234 °C.  $C_{39}H_{37}BN_8O_3SZn$  (774.0): calcd: C 60.52, H 4.82, N 14.48, S 4.14; found C 60.39, H 4.66, N 14.70, S 4.38.  $^1H$  NMR ( $CDCl_3$ ):  $\delta$  = 0.17 [t,  $J$  = 6.9 Hz, 3 H,  $CH_3(Et)$ ], 2.57 [s, 9 H, Me(pz)], 2.72 [q,  $J$  = 6.9 Hz, 2 H,  $CH_2(Et)$ ], 6.19 [s, 3 H, H(pz)], 6.78 (m, 2 H,  $C_6H_4$ ), 7.37 (m, 9 H, Ph), 7.65 (m, 6 H, Ph), 8.12 (m, 2 H,  $C_6H_4$ ).

**Structure Determinations:**<sup>[35]</sup> All crystals were obtained as described above from the reaction solutions. Diffraction data were recorded at 180 K (1 at room temp.) on a Bruker Smart CCD diffractometer and subjected to an empirical absorption correction (program SADABS). The structures were solved with direct methods and refined anisotropically with the SHELX program suite.<sup>[36]</sup> Hydrogen atoms were included with fixed distances and isotropic temperature factors 1.5 times those of their attached atoms. Parameters were refined against  $F^2$ . The  $R$  values are defined as  $R_1 = \Sigma|F_o - F_c|/\Sigma F_o$  and  $wR_2 = \{\Sigma[w(F_o^2 - F_c^2)]^2/\Sigma[w(F_o^2)]^2\}^{1/2}$ . Drawings were produced with SCHAKAL.<sup>[37]</sup> Table 1 lists the crystallographic data.

## Acknowledgments

This work was supported by the Deutsche Forschungsgemeinschaft and the Fonds der Chemischen Industrie. We are indebted to Mrs. Petra Klose for technical assistance and to Drs. Werner Deck and Alexander Trösch for help with the crystallography.

- [1] *Bioinorganic Chemistry* (Eds.: I. Bertini, H. B. Gray, S. J. Lipard, J. S. Valentine), University Science Books, Mill Valley, California, **1994**.
- [2] W. Kaim, B. Schwederski, *Bioanorganische Chemie*, Teubner Studienbücher, Stuttgart, **1995**.
- [3] *Carbonic Anhydrase* (Eds.: F. Botrè, G. Gros, B. T. Storey), VCH Publishers, Weinheim, **1991**.
- [4] For the literature up to 1982, see: R. S. Brown, J. Huguet, N. J. Curtis, in *Metal Ions in Biological Systems* (Ed.: H. Sigel), Vol. 15, Marcel Dekker, New York, **1983**.
- [5] For more recent references, see G. Parkin, *Adv. Inorg. Chem.* **1995**, *42*, 291–393.
- [6] R. Alsasser, M. Ruf, S. Trofimenko, H. Vahrenkamp, *Chem. Ber.* **1993**, *126*, 703–710.
- [7] M. Ruf, H. Vahrenkamp, *Inorg. Chem.* **1996**, *35*, 6571–6578.

- [8] M. Ruf, F. A. Schell, R. Walz, H. Vahrenkamp, *Chem. Ber./Recueil* **1997**, *130*, 101–104.
- [9] A. Trösch, H. Vahrenkamp, *Inorg. Chem.* **2001**, *40*, 2305–2311.
- [10] For a summary of references, see S. Sinnecker, M. Bräuer, W. Koch, E. Anders, *Inorg. Chem.* **2001**, *40*, 1006–1013.
- [11] H. Vahrenkamp, *Acc. Chem. Res.* **1999**, *32*, 589–596.
- [12] M. Bräuer, E. Anders, S. Sinnecker, W. Koch, M. Rombach, H. Brombacher, H. Vahrenkamp, *Chem. Commun.* **2000**, 647–648.
- [13] M. Rombach, C. Maurer, K. Weis, E. Keller, H. Vahrenkamp, *Chem. Eur. J.* **1999**, *5*, 1013–1027.
- [14] M. Rombach, H. Vahrenkamp, *Inorg. Chem.* in print.
- [15] U. Brand, M. Rombach, J. Seebacher, H. Vahrenkamp, *Inorg. Chem.* in print.
- [16] H. Brombacher, H. Vahrenkamp, work in progress.
- [17] A. G. Looney, R. Han, I. B. Gorell, M. Cornebise, K. Yoon, G. Parkin, A. L. Rheingold, *Organometallics* **1995**, *14*, 274–284.
- [18] W. Kläui, U. Schilde, M. Schmidt, *Inorg. Chem.* **1997**, *36*, 1598–1601.
- [19] N. A. Bell, P. T. Moseley, H. M. M. Shearer, C. B. Spencer, *Acta Crystallogr., Sect. B* **1980**, *36*, 2950–2954.
- [20] R. Han, G. Parkin, *J. Am. Chem. Soc.* **1991**, *113*, 9707–9708.
- [21] H. C. Böttcher, M. Graf, K. Merzweiler, C. Wagner, *Z. Anorg. Allg. Chem.* **2000**, *626*, 597–603.
- [22] M. Bonamico, G. Dessy, V. Fares, L. Scaramuzza, *J. Chem. Soc., Dalton Trans.* **1972**, 2515–2517.
- [23] J. A. McCleverty, N. J. Morrison, N. Spencer, C. C. Ashworth, N. A. Bailey, M. R. Johnson, J. M. A. Smith, B. A. Tabbiner, C. R. Taylor, *J. Chem. Soc., Dalton Trans.* **1980**, 1945–1957.
- [24] M. Ruf, K. Weis, H. Vahrenkamp, *Inorg. Chem.* **1997**, *36*, 2130–2137.
- [25] M. A. Romero, M. P. Sanchez, M. Quiros, F. Sanchez, J. M. Salas, M. N. Moreno, R. Faure, *Can. J. Chem.* **1993**, *71*, 29–33.
- [26] M. L. Godino-Salido, M. D. Gutierrez-Valero, R. Lopez-Garzon, J. M. Moreno-Sanchez, *Inorg. Chim. Acta* **1994**, *221*, 177–181.
- [27] R. S. Hosmane, B. B. Lim, *Tetrahedron Lett.* **1985**, *26*, 1915–1918. W. Walter, K. J. Reubke, *Chem. Ber.* **1969**, *102*, 2117–2128.
- [28] E. Anders et al. and H. Vahrenkamp et al., work in progress.
- [29] C. Bergquist, H. Storrie, H. Koutcher, B. M. Bridgewater, R. A. Friesner, G. Parkin, *J. Am. Chem. Soc.* **2000**, *122*, 12651–12658.
- [30] R. Alsasser, A. K. Powell, S. Trofimenko, H. Vahrenkamp, *Chem. Ber.* **1993**, *126*, 685–694.
- [31] D. L. Greene, B. J. McCormick, C. G. Pierpont, *Inorg. Chem.* **1973**, *12*, 2148–2152.
- [32] M. Förster, R. Burth, A. K. Powell, T. Eiche, H. Vahrenkamp, *Chem. Ber.* **1993**, *126*, 2643–2648.
- [33] M. Ruf, R. Burth, K. Weis, H. Vahrenkamp, *Chem. Ber.* **1996**, *129*, 1251–1257.
- [34] E. Fluck, F. Horn, *Synth. Inorg. Met. Org. Chem.* **1972**, *2*, 341–343.
- [35] The crystallographic data of the structures described in this paper were deposited with the Cambridge Crystallographic Data Centre as supplementary publication no. CCDC – 166856 for **1**, 166855 for **3**, 166954 for **4**, 166857 for **5c**, 166859 for **6a**, 166860 for **7** and 166858 for **8**. Copies of these data are available free of charge from the following address: The Director, CCDC, 12 Union Road, Cambridge, CB2 1EZ, UK [Fax: (internat.) +49–1223/336–033; E-mail: deposit@ccdc.cam.ac.uk].
- [36] G. M. Sheldrick, *SHELX-86* and *SHELXL-93*, *Programs for Crystal Structure Determination*, Universität Göttingen, **1986** and **1993**.
- [37] E. Keller, *SCHAKAL for Windows*, Universität Freiburg, **1998**.

Received July 10, 2001

[I01257]